ELSEVIER

Polymer 44 (2003) 261–275

polymer

www.elsevier.com/locate/polymer

Toughening of polypropylene with calcium carbonate particles

W.C.J. Zuiderduin, C. Westzaan, J. Huétink, R.J. Gaymans*

Department of Chemical Technology, University of Twente, P.O. Box 217, 7500 AE Enschede, The Netherlands

Received 25 July 2002; received in revised form 4 October 2002; accepted 22 October 2002

Abstract

Polypropylene–$CaCO_3$ composites were prepared on a twin screw extruder with a particle content of 0–32 vol%. The influence of particle size (0.07–1.9 μm) and surface treatment of the particles (with and without stearic acid) on the toughening properties were studied. The matrix molecular weight of the polypropylene was also varied (MFI 0.3–24 dg/min). The experiments included tensile tests, notched Izod impact tests, differential scanning calorimetry (DSC), scanning electron microscopy and rheology experiments. The modulus of the composites increased, while the yield stress was lowered with filler content. This lowering of yield stress was connected to the debonding of the particles from the polypropylene matrix. From DSC experiments it was shown that the particle content had no influence on the melting temperature or crystallinity of the PP phase, also particle size showed no effect on the thermal properties. The impact resistance showed large improvement with particle content. The brittle-to-ductile transition was lowered from 90 to 40 °C with the addition of $CaCO_3$ particles. Notched Izod fracture energy was increased from 2 up to 40–50 kJ/m^2. The stearic acid coating on the particle surface showed a large positive effect on the impact strength. This was mainly due to the improved dispersion of the $CaCO_3$ particles. Aggregates of particles clearly had a detrimental effect on the impact behaviour of the composites. The smaller particle sizes (<0.7 μm) showed coarse morphologies and this lowered the toughening efficiency. The molecular weight of the polypropylene matrix had a profound effect on the toughening properties. A higher molecular mass shifted the brittle-to-ductile transition towards lower temperatures. At the higher filler loads (>20 vol%), however, still problems seem to occur with dispersion, lowering the toughening efficiency. Of all particle types used in this study the stearic acid treated particles of 0.7 μm were found to give the best combination of properties. From the study of the micro-toughening mechanism it was shown that at low strain the particles remain attached to the matrix polymer. At higher strain the particles debond and this leads to a change in stress state at the particle size level. This prevents crazing of the matrix polymer and allows extensive plastic deformation, resulting in large quantities of fracture energy.

Keywords: Impact strength; Toughening; Rigid particles

1. Introduction

The purpose of adding mineral fillers to polymers was primarily one of cost reduction. In recent years, however, the fillers are more often used to fulfil a functional role, such as increasing the stiffness or improve the dimension stability of the polymer [1].

The mineral fillers used in semi-crystalline polymers are usually talc and calcium carbonate and, to a lesser extend mica and wollastonite [2]. Generally, the addition of mineral fillers will have an embrittling effect on polymers and decrease the impact energy [1]. In fact most of the studies on modification of semi-crystalline polymers with rigid particles report a significant loss of toughness compared to the neat polymer.

A new concept is the usage of filler particles as toughening agent [3]. The general idea behind this study is to mimic the rubber toughening mechanism using rigid filler particles. The rigid particles must debond and create free volume in the blend on a sub-micron size level. This is much like the cavitation mechanism in rubber toughened systems. The micro-mechanistic model for this toughening effect is shown in Fig. 1. The micro-mechanism consists of three stages:

I *Stress concentration*. The modifier particles act as stress concentrators, because they have different elastic properties compared to the matrix polymer.

II *Debonding*. Stress concentration gives rise to built up of triaxial stress around the filler particles and this

---

* Corresponding author. Tel.: +31-53-4892970.
E-mail address: r.j.gaymans@ct.utwente.nl (R.J. Gaymans).

0032-3861/03/$ - see front matter © 2002 Elsevier Science Ltd. All rights reserved.
PII: S0032-3861(02)00769-3

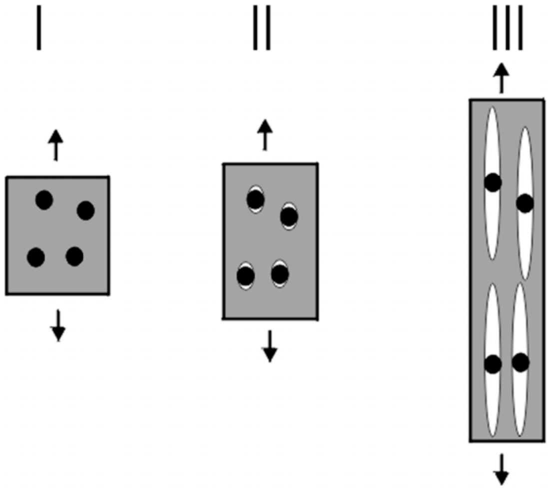

Fig. 1. Toughening mechanism with rigid particles [3].

leads to debonding at the particle–polymer interface.

III *Shear yielding*. The voids caused by debonding alter the stress state in the host matrix polymer surrounding the voids. This reduces the sensitivity towards crazing since the volume strain is released. The shear yielding mechanism becomes operative and the material is able to absorb large quantities of energy upon fracture.

In order for rigid filler particles to act as toughners, they must fulfil certain requirements.

- The particles should be of small size (less then 5 μm) otherwise the voids that are created would act as initiation sites for the fracture process. The creation of stable free volume is what is desired.
- The aspect ratio must be close to unity to avoid high stress concentrations.
- The particles must debond prior to the yield strain of the matrix polymer in order to change the stress state of the matrix material.
- The particles must be dispersed homogeneously in the matrix polymer, aggregation should be avoided.

There are a few cases, which report an increase in impact resistance upon addition of a rigid filler. For polyethylene Wang et al. [5], Hoffmann et al. [6], Badran et al. [7], Bartzack et al. [1] and Liu et al. [8] showed an impressive impact improvement with the addition of rigid particles.

For polypropylene, it was already known that a moderate impact improvement with rigid particles was possible, as found by Pukánszky et al. [2] and Baker et al. [4] and recently this was confirmed by Thio and Argon [9]. The fracture mode, however, still was in a brittle fashion in these studies no full plastic deformation was found; the fracture energies were limited to 2–8 kJ/m^2. Complete toughened systems of polypropylene with $CaCO_3$ with notched fracture energies rising to 40–50 kJ/m^2 were reported by our group previously [10]. Polyketone polymers toughened with $CaCO_3$ were also reported previously with complete ductility at room temperature and notched impact strength of 80 kJ/m^2 [11].

A mineral filler can profoundly change the characteristics of a polymer system. The properties of the particles themselves (size, shape and modulus) can have a significant effect, especially on the deformation behaviour. The heterogeneous phase can also change the structure of the matrix polymer. The particle can act as a nucleating agent for crystallisation or decrease the crystallinity by introducing kinetic hindrance [12]. Reduced mobility of polymer chains by kinetic hindrance leads to the development of small and imperfect crystallites, forming a crystalline phase of low heat of fusion [13,14]. Transcrystallinity can be introduced in polymers by crystallisation from the particle surface [15]. The transcrystalline layer has other properties compared to the spherulitic form, in the case of PP the transcrystalline layer possesses higher rigidity and lower deformability, which leads to earlier crack initiation and crack propagation [16,17].

Introduction of fillers into a polymer matrix results in a heterogeneous system. Under effect of external load these heterogeneities induce stress concentration, the magnitude of which depends on the geometry of the particles [18,19]. With anisotropic particles the stress concentration that develops can be significantly large at the edges or the end of the particles. Stress concentration increases with increasing aspect ratio [20].

The $CaCO_3$ particles are generally supplied as agglomerates and during processing these aggregates have to be broken up and dispersed in to the primary particles. Large particle–particle interactions result in inhomogeneous distribution of the filler, processing problems, poor appearance and inferior properties. The two major factors, which determine the particle–particle interactions, are particle size and surface free energy [2]. The effects of aggregates on the properties of composites are clearly detrimental. Many authors emphasise this fact together with the importance of best possible homogeneity [20–23]. Increasing amounts of aggregates lead to a drastic decrease of impact resistance of polymer composites [28,29].

Adsorption of polymer molecules on the filler surface leads to the development of an interphase layer, which has properties different from those of the matrix polymer [25–28]. Changes in interfacial interactions between particles and matrix polymer can modify the debonding mechanism, failure behaviour and thus, the overall performance of composites. The most used technique to change the particle–particle and polymer–particle interactions is the coverage of filler surface with a low molecular weight organic compound [13,24,25,29]. For $CaCO_3$ often stearic acid is used [21,29,30]. The surfactant molecules are coupled with ionic bonds to the filler surface and the stearic acid molecules are oriented in directions normal to the surface [31]. As a result of the surface coating the surface free energy of the filler decreases dramatically [30,32].

Approximately 210 mJ/m^2 surface tension of a $CaCO_3$ filler can be reduced to 40–50 mJ/m^2 by stearic acid treatment [2]. Filler treatment with a stearic acid reduces the particle–particle interaction and this will lead to a better dispersion of the particles in the host matrix polymer. Also the polymer–particle adhesion is lowered when a surfactant is used, and this has consequences for the debonding properties of the composite. When the adhesion is low debonding can occur and as a result crazing is suppressed and the yield mechanism becomes operative [30]. Plastic deformation of the matrix polymer is the main energy absorbing process in impact and this increases when the interaction between particles and polymer is lowered [19,33,34].

A commonly accepted view on the role of filler particles is that debonding alters the stress state in the material around the particles and induce extensive plastic deformation in the matrix, such as multiple crazing [35–37], shear yielding [38,39], crazing with shear yielding [40–42] and rubber particle stretching or tearing and debonding at the inorganic filler particle [43–45].

1.1. Aim

In this paper, the toughening of polypropylene with calcium carbonate particles is studied. The aim is to mimic the micro-mechanism of rubber cavitation followed by shear yielding of the matrix polymer with rigid particles. In this manner a material can be developed in which an increased stiffness can be combined with an increased fracture resistance. Several $CaCO_3$ particles will be studied, which have different particle sizes and surface treatment. The influence of matrix molecular weight on the toughening behaviour was also evaluated.

2. Experimental

2.1. Materials

Commercially available polypropylene and precipitated calcium carbonates were kindly supplied by DSM and Mineral technologies. Material specifications are listed in Table 1. Unless otherwise stated the PP is used with a MFI of 2.4 dg/min and $CaCO_3$ particle Type A.

2.2. Specimen preparation

Compounding of the materials was done using a Berstorff (ZE 25 × 33D) twin screw extruder. In the extrusion step, barrel temperatures were set at 195/210/200/200/200/200/200 °C and a screw speed of 140 rpm was used. The L/D ratio of the screws was 33, and $D = 25$ mm.

After compounding, the blends were injection moulded into rectangular bars (74 × 10 × 4 mm^3) and dumbbell shaped specimen using an Arburg Allrounder 221-55-250 injection moulding machine. The barrel had a flat temperature profile of 220 °C, the mould temperature was kept at 40 °C with an injection pressure of 55 bar, holding pressure was kept at 45 bar.

A single-edge V-shaped notch of 2 mm depth and tip radius 0.25 mm was milled in the moulded specimens for the notched Izod impact experiments.

2.3. Scanning electron microscopy

Scanning electron microscopic (SEM) pictures were taken to study the morphology of the $CaCO_3$ composites. Samples were taken from the core of the injection moulded bars. SEM specimens were prepared by cutting with a CryoNova microtome at −120 °C using a diamond knife (−110 °C) and cutting speed of 1 mm/s. The cut surfaces were then sputter-coated with a thin gold layer and studied with Hitachi S-800 field emission SEM.

2.4. Conditioning

The test bars were dried at 80 °C under vacuum for 15 h, and kept under vacuum at room temperature after this drying step.

2.5. Notched Izod impact test

Notched Izod impact tests were carried out using a Zwick pendulum. To vary the test temperature, the specimens were placed in a thermostatic bath. The impact strength was calculated by dividing the absorbed energy by the initial cross-sectional area behind the notch (32 mm^2). All measurements were carried out in ten-fold.

Table 1
Material properties

Material	Designation	Supplier	Coating	Description
Vestolen P grade	PP	Currently DSM (Former Vestolen GmbH)	–	T_m: 170 °C, T_g: 10 °C, crystallinity: 45 wt%, MFI: 2.4 dg/min.
Superpflex	Type A	Minerals technologies	Yes	Particle size 0.7 μm
Albafil	Type B	Minerals technologies	No	Particle size 0.7 μm
Multifex	Type C	Minerals technologies	No	Particle size 0.07 μm
Ultrafex	Type D	Minerals technologies	Yes	Particle size 0.07 μm
Tuffguard	Type E	Minerals technologies	Yes	Particle size 0.3 μm
Albacar	Type F	Minerals technologies	No	Particle size 1.9 μm

2.6. DSC

Differential scanning calorimetry (DSC) spectra were recorded on a Perkin Elmer DSC7 apparatus, equipped with a PE7700 computer and Tas-7 software. Two to five milligrams of dried sample was heated at a rate of 20 K/min. The peak temperature of the second scan was taken as the melting temperature of the polymer; the peak area was used to determine the melting enthalpy.

2.7. Tensile tests

Standard tensile tests were conducted on dumbbell shaped specimens with a Zwick tensile tester type ZO2, all tests were carried out in five folds. Extensometers were used to measure the strain during the tensile test. Test speed was kept at 60 mm/min ($1.25 \times 10^{-2}\ s^{-1}$). During the test the force was recorded versus nominal strain.

2.8. Melt viscometry

In this experiment, the viscosity is monitored in time at a temperature of 270 °C. A Kayeness Galaxy V was used to monitor the melt viscosity in time. The cylinder had a diameter of 9.5 mm and the capillary had a diameter of 1 mm and a length of 1 mm. The cylinder was kept at a temperature of 270 °C, the cylinder was filled with polymer and compressed to remove the trapped air. The Piston speed was kept at 1 mm/min during the experiment. After 5 min the experiments were started. The force was measured every 30 s, up to 20 min.

3. Results and discussion

3.1. Effect of particle content

The particle content is usually given in volume fraction. Table 2 compares the weight fraction and volume fraction of the filler particles used in this paper.

3.1.1. Introduction

A series of composites was studied with composition varying from 0 up to 31.5 vol% $CaCO_3$ particles. The particle size used in this series was 0.7 μm, with a narrow particle size distribution. The particles had been treated with a stearic acid to cover the surface of the filler (Type A particles). The particle morphology is shown in Fig. 2. The $CaCO_3$ particles have an aspect ratio close to unity. The particles do not have sharp edges or show large size differences.

Table 2
Particle content in weight and volume percentage, PP–$CaCO_3$

Particle content (wt%)	Particle content (vol%)
0	0
10	3.60
20	8.10
30	13.1
40	19.0
50	25.0
60	34.5

3.1.2. Morphology

The morphology of the compounds up to a concentration of 60 wt% $CaCO_3$/stearic acid coated particles is shown in Fig. 3. The morphology consists of finely dispersed particles in the polypropylene matrix. The aggregates are broken up to the primary particles during the extrusion process. The interparticle distance is lowered with increasing particle content as expected. The obtained particle size is approximately 0.7 μm. No large aggregates are present, this morphology is optimal for toughening to occur.

3.1.3. Melt viscosity

This experiment is used to determine the melt stability of polymers. Polypropylene is quite stable in the melt, but at higher temperatures and high shear rates a viscosity decrease is observed [46]. The influence of the filler particles on the chain scission behaviour was studied using a capillary rheometer. The polymer melt was monitored in time, a steady flow through a small capillary was maintained and the force necessary was measured. The results are shown in Fig. 4.

The $CaCO_3$ particles have no influence on the matrix viscosity, the melt of filled polypropylene does not show extensive degradation. The melt viscosity of PP is known to reduce when degradation takes place, no sign of chain scission or molecular weight loss was found in this study.

3.1.4. Thermal properties

The concentration of the $CaCO_3$/stearic acid coated

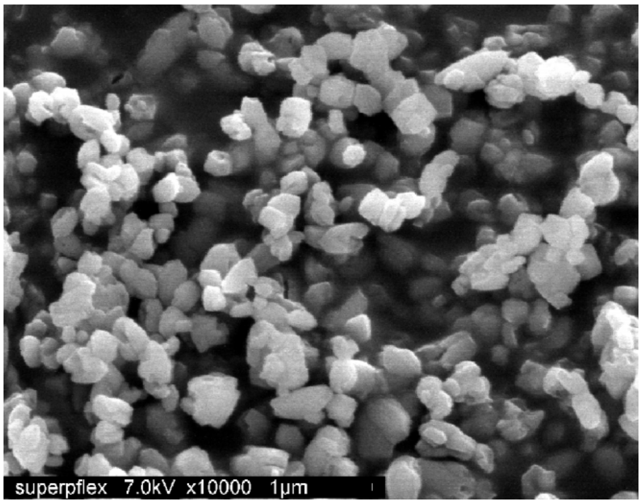

Fig. 2. Scanning electron microscopic image of $CaCO_3$ particles, coated particles (Type A).

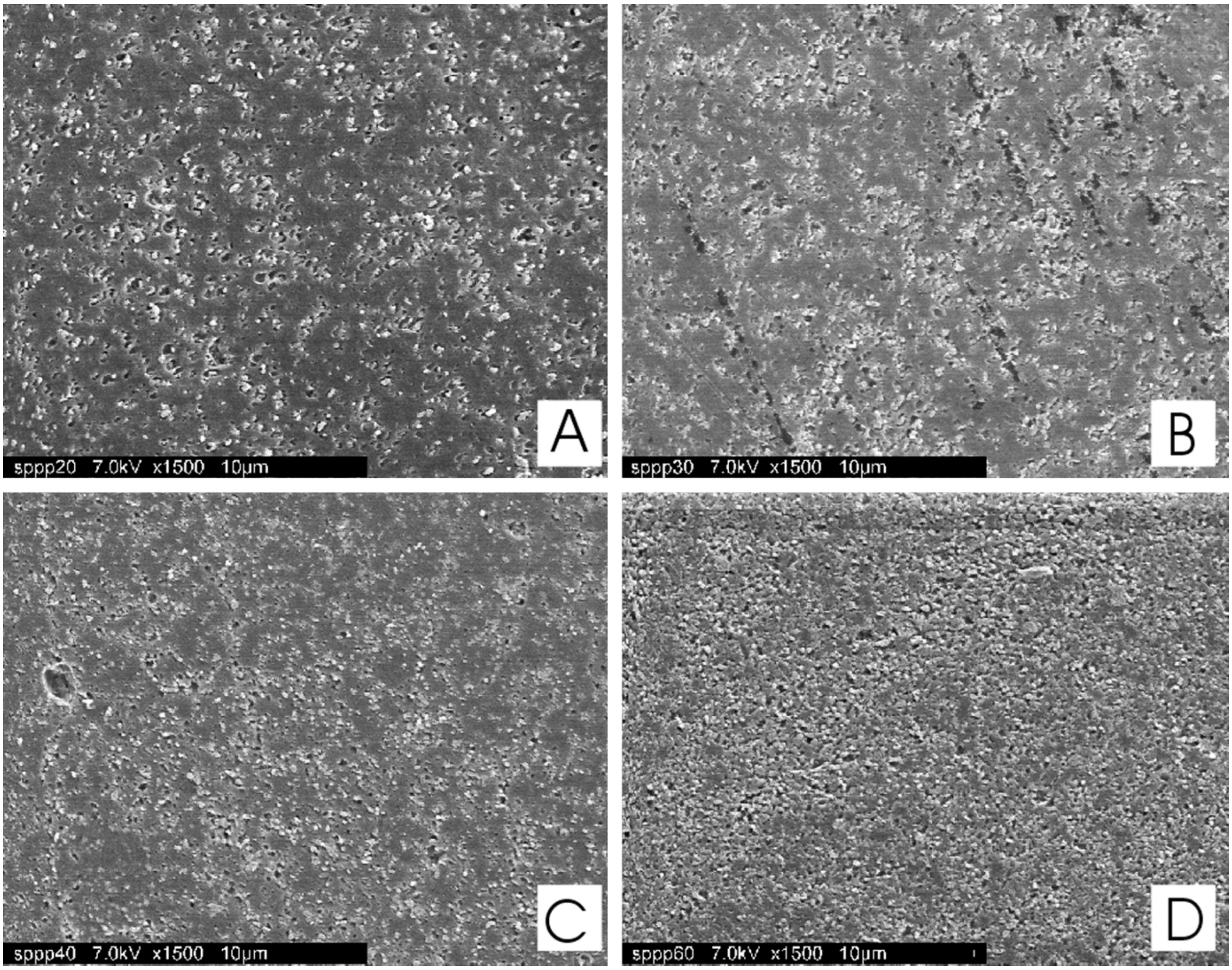

Fig. 3. Scanning electron microscope images of morphology of PP–$CaCO_3$ composites, Type A particles; (A) 20 wt%; (B) 30 wt%; (C) 40 wt%; (D) 60 wt%.

particles had no influence on the melting temperature (Fig. 5). The melt enthalpy (corrected for the filler load) is constant up to a filler load of 40 wt%. The highest filler concentration (60 wt%) does give a small lowering of the melt enthalpy; this may be due to a lowering of the mobility of the polymer chains at this high filler load. The $CaCO_3$/stearic acid coated particles do not act as a nucleating species in polypropylene since the crystallinity is not increased. This is as expected as the stearic acid lowers the surface energy of the $CaCO_3$ particles and therefore cannot act as a strong nucleating species. The interaction of the polymer chains with the particles is lowered due to the coating on the $CaCO_3$ particles.

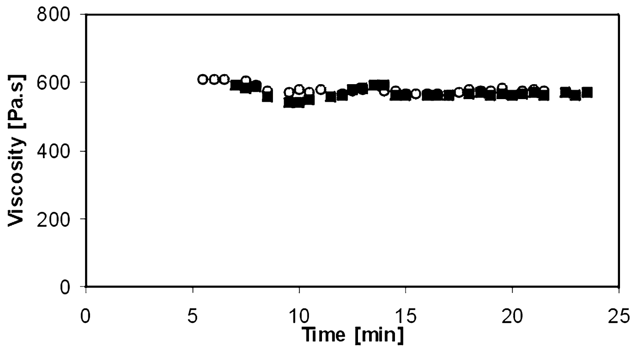

Fig. 4. Melt viscosity as function of time, PP–$CaCO_3$ composites, 270 °C, piston speed 1 mm/min, ○, PP; ■, PP–40 wt% $CaCO_3$.

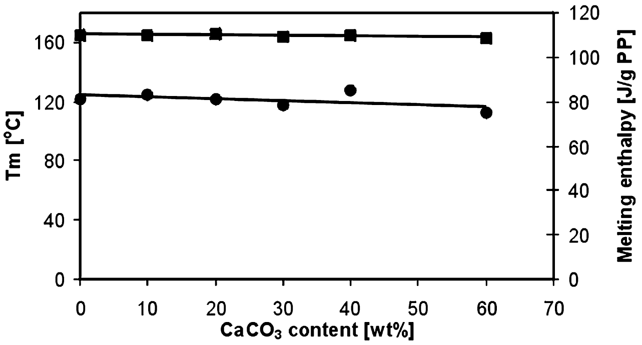

Fig. 5. Melting temperature and melting enthalpy as a function of particle content, DSC, 20 °C/min. ■, Melting temperature; ●, Melting enthalpy.

3.1.5. Tensile properties

The tensile properties are shown in Figs. 6 and 7. The modulus of the system is increasing with particle content. The stiffness is increased from 1840 to 2700 MPa by adding 19 vol% of $CaCO_3$ to the polymer, which is an increase of 46%. Obviously, the particles do not debond at these low strains. The modulus increase with volume fraction of rigid filler is somewhat lower compared to what is predicted by the relationship of Einstein–Guth. The polypropylene–EPDM blend shows a considerable decrease in stiffness in this filler load regime. At low strains the PP–$CaCO_3$ composites are clearly superior.

The yield stresses are plotted as a function of particle concentration at different temperatures in Fig. 7; it is clearly demonstrated that the yield stress is decreased upon addition of the $CaCO_3$ particles. It should be noted that the yield stress is also decreased at temperatures below the glass transition of the matrix polymer (10 °C). The yield stress is decreased linearly with $CaCO_3$ concentration over the entire temperature range. The decrease of the yield stress must be due to the debonding of the filler particles from the matrix polymer. Debonded particles do not contribute to the yield stress. With the 30 wt% compound (13.1 vol%) the yield stress drops to 28.8 MPa which is a lowering of 18.6%. At higher filler content the decrease in yield stress is not as strong as observed with rubber particles (Fig. 8). At the lowest temperature of − 50 °C the decrease of yield stress is less pronounced, this suggests that at this temperature not all the particles debond from the matrix (Fig. 7).

3.1.6. Impact resistance

The debonding of the particles creates free volume at the particle size level and therefore the stress state is altered in the vicinity of the particles. This mechanism is similar to that of cavitation in rubber toughened blends. The debonding is necessary otherwise no impact improvement can be expected. The notched Izod fracture energies as a function of temperature are shown in Fig. 9.

The fracture energy of the ductile fractures is approximately 45 kJ/m^2. This is in accordance with what was found with rubber toughened blends [46]. This large energy consumption stems from the shear yielding of the matrix polymer. The debonding of the rigid inclusions does not consume large quantities of energy but is necessary to suppress crazing of the matrix polymer. The fracture energy at room temperature is increased considerably when $CaCO_3$ is added to the polypropylene matrix (Fig. 10). The impact resistance is increased by a factor four by adding 60 wt% (34.5 vol%) $CaCO_3$. The modulus is at the same time increased from 1840 to 4380 MPa. The brittle-to-ductile transition is shifted towards lower temperatures with increasing $CaCO_3$ content (Fig. 9). It is shown in Fig. 11 that the rigid particles are as effective as the rubber particles up to 15 vol% particles. With the rubber blends, the T_{bd} is lowered far below the glass transition temperature while the compounds with $CaCO_3$ particles do not show a further lowering of the T_{bd} below 40 °C.

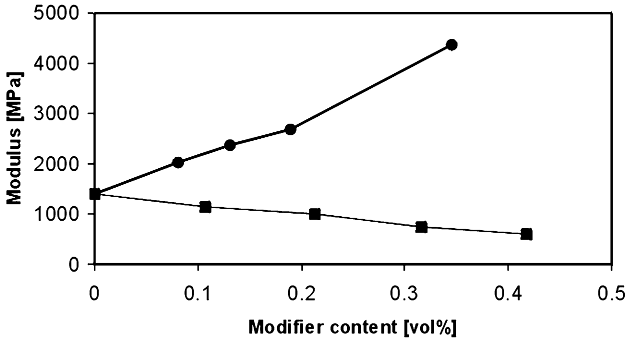

Fig. 6. Modulus as a function of $CaCO_3$ content, tensile, 20 °C, 60 mm/min; ■, PP–EPDM [51]; ●, PP–$CaCO_3$.

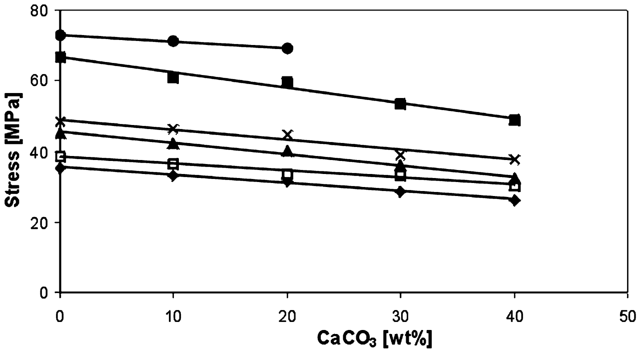

Fig. 7. Yield stress as function of $CaCO_3$ (Type A) content, tensile, 60 mm/min; ●, − 50 °C; ■, − 30 °C; ×, − 10 °C; ▲, 0 °C; □, 10 °C; ◆, 20 °C.

The highest concentration (60 wt%) shown here does not lead to a further lowering of the T_{bd}. This could be due to a difficulty in dispersing the particles at 60 wt%. The particles will be more agglomerated in that case; larger aggregates will lead to more brittle behaviour. This is in accordance with what was found in literature [16,45]. The free volume that is created by the debonding step will in that case be less stable. The voids will be of a larger size and may lead to crack initiation.

The glass transition of the matrix polymer is not expected to be the limit for toughening as shown in Fig. 11; the particles are still debonding from the matrix below the

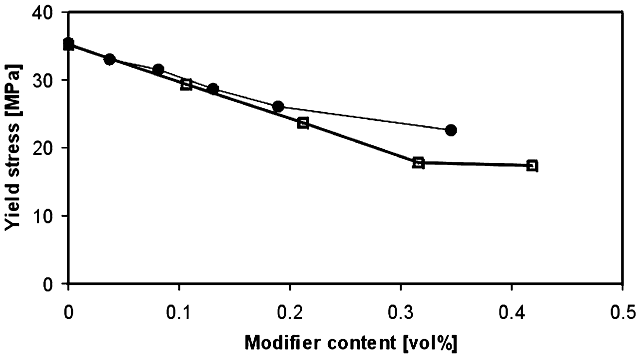

Fig. 8. Yield stress as function of modifier content, □, PP–EPDM [51]; ●, PP–$CaCO_3$; tensile, 60 mm/min, 20 °C.

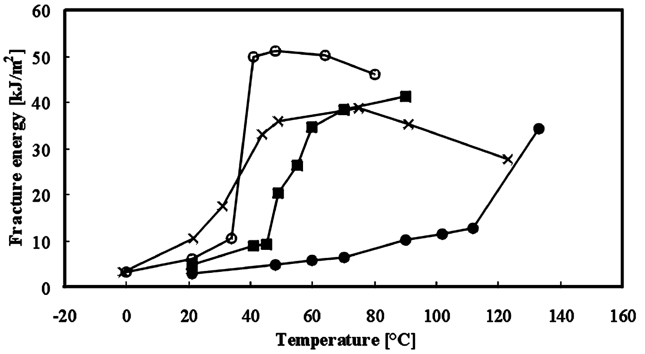

Fig. 9. Fracture energy as a function of temperature for PP–$CaCO_3$ composites with different filler content; ●, PP; ■, 20 wt%; ○, 40 wt%; ×, 60 wt%.

matrix glass transition temperature and the yield stress is still decreasing. Furthermore with rubber toughening it has been shown that the toughening can be effective well below the glass transition of the matrix polymer [47,48].

3.1.7. Fracture micro-mechanism

One of the striking aspects of the deformation behaviour of polymer/rubber blends is the occurrence of stress whitening in deformed samples. Stress whitening is linked to the ductile responds of the blend. It was demonstrated by Ramsteiner [49] that stress whitening in rubber blends could be attributed to the cavitation of rubber particles. Gaymans et al. [50] showed that near the fracture surface the cavities were strongly deformed. Speroni and coworkers [51] demonstrated that at a larger distance from the fracture surface still voids were present, and that the deformation of these voids was a function of the distance from the fracture plane. Oostenbrink et al. [52] demonstrated that the deformation at high strain rates may be divided into three layers. At a large distance from the fracture surface a zone is visible where the particles are cavitated but the voids are not deformed. Closer to the fracture plane the voids become strongly deformed, and have ellipsoid shapes. Directly beneath the fracture surface is a third zone where no cavitation and deformation is visible. The authors suggest that local heating around the fast running crack tip had been large enough to form a melt layer in the material. A similar effect has been reported by Boode [53], who found a practically undeformed layer beneath the fracture plane in ABS samples deformed in an Izod impact test.

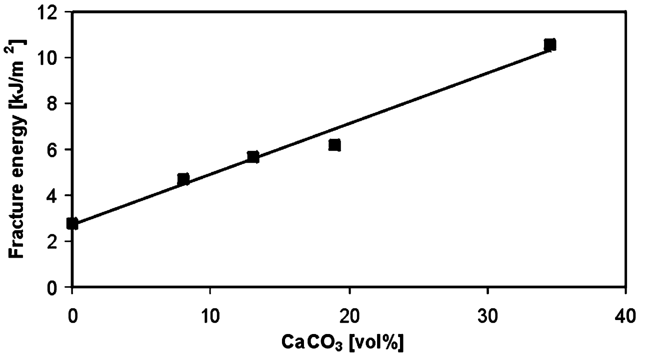

Fig. 10. Notched Izod fracture energy as function of $CaCO_3$ content, 20 °C.

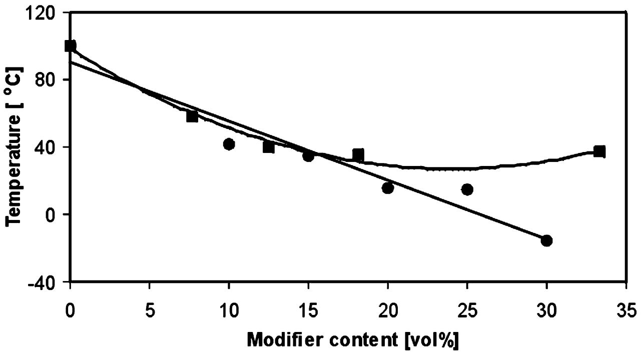

Fig. 11. Brittle-to-ductile transition temperatures as a function of particle content; ■, PP–$CaCO_3$; ●, PP–EPDM [20].

The scanning electronic microscopy image shown in Fig. 12 shows the deformation morphology after fracture below the fracture plane of a ductile fractured notched Izod sample (13.1 vol% $CaCO_3$). The crack has run from left to right.

The voids present in the material near the fracture surface are elongated due to the deformation of the surrounding host matrix polymer (Fig. 12). The voids show strong deformation, this is reflected in the aspect ratio of the cavities. The aspect ratio of the voids is a measure for the plastic strain of the matrix polymer next to the voids. The deformation of the matrix polymer is quite large; the thin ligaments show strains well above the natural draw ratio of the polypropylene.

The voids formed by debonding are stable in the sense that they do not coalescence with each other. This is an important feature of the fracture mechanism; if the cavities grow to a too large size they could initiate early fracture of the material. The deformation is lowered if the distance to the fracture plane is increased. Next to the fracture surface a layer without cavities is present (Fig. 12(B) and (D)). This suggests that the cavities are relaxed after fracture. The relaxation of strong deformation can take place in the melt of the material or by means of mechanical melting or relaxation due to the large thermal effects and elastic recovery [54,55].

4. Influence of particle coating on properties of PP composites

4.1. Introduction

To study the influence of a stearic acid coating on $CaCO_3$ particles dispersed into a host matrix, two identical particle sizes were chosen, one with (Type A) and one without stearic acid (Type B) applied to the surface of the particle. The coating could influence the properties of the composites.

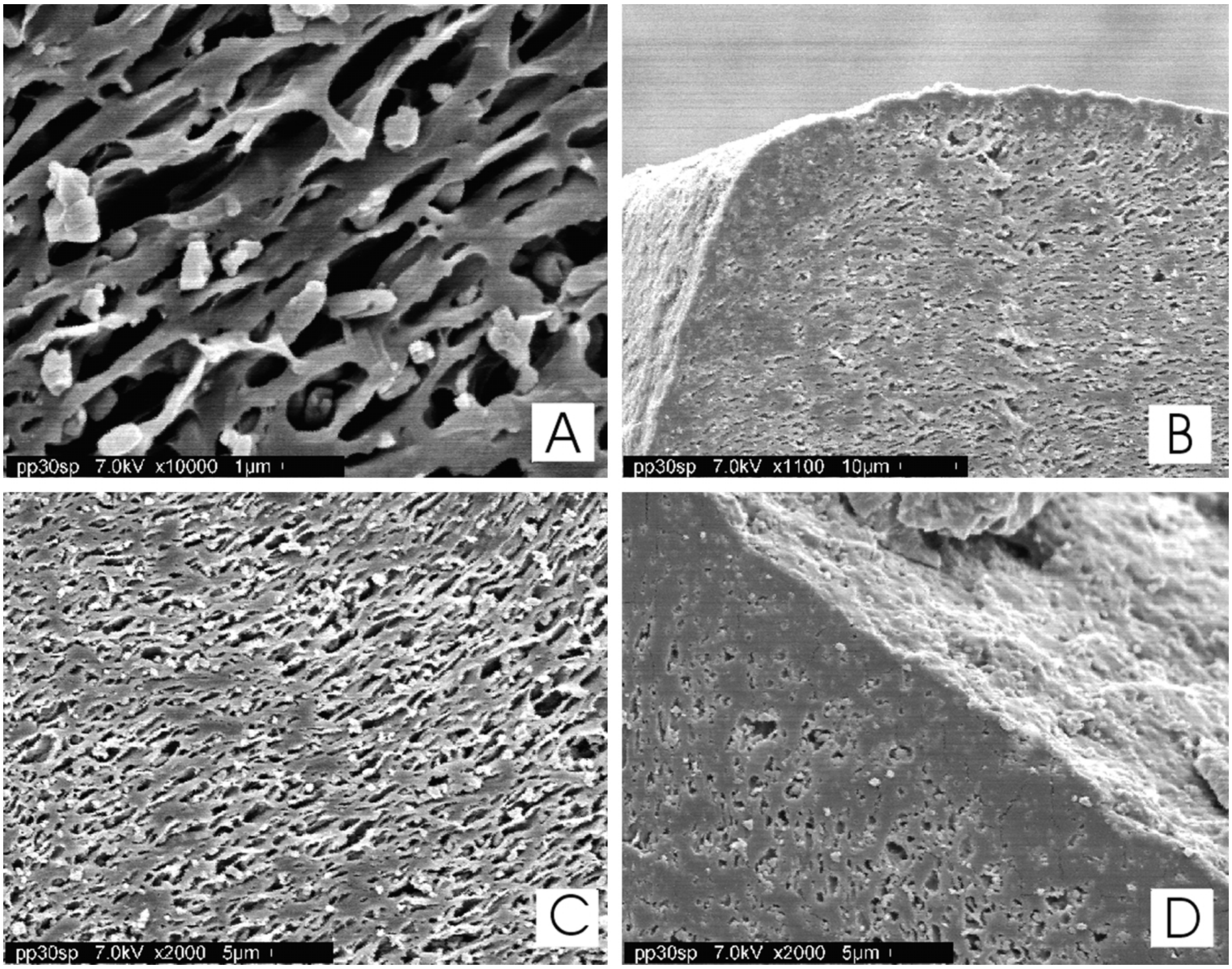

Fig. 12. SEM images in the deformation zone perpendicular to the fracture surface of PP–$CaCO_3$ composites, 30 wt% (13.1 vol%). The crack direction was from left to right, samples taken from center of fractured notched Izod specimen: (A) and (C) 30 μm below fracture surface; (B) and (D) directly below fracture surface.

4.2. Viscosity experiments

The rate of decrease of the viscosity is a relative measure for the degradation process. The results are shown in Fig. 13.

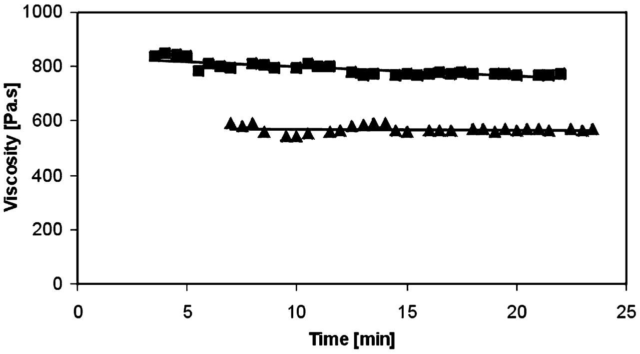

Fig. 13. Melt viscosity of PP composites, ■, 30 wt% untreated $CaCO_3$; ▲, 30 wt% treated $CaCO_3$.

The viscosity decreases a little for both the composites with treated and the untreated $CaCO_3$ particles. The melt degradation is not crucial for these types of composites. The organic coating on the surface of the filler particle lowers the melt viscosity of the composite significantly. The adhesion between particle and polymer is lowered when a stearic acid coating is present as well as the particle–particle interaction.

4.3. Composite morphology

The dispersion of the particles is very important for the toughening properties. The morphology of the composites with stearic acid treated particles were shown in Fig. 3. The morphology of the composites with uncoated particles shows a much coarser structure (Fig. 14). There are still aggregates present; dispersion obviously is more difficult for the untreated particles. The particle–particle interaction is larger due to the higher surface free energy. These

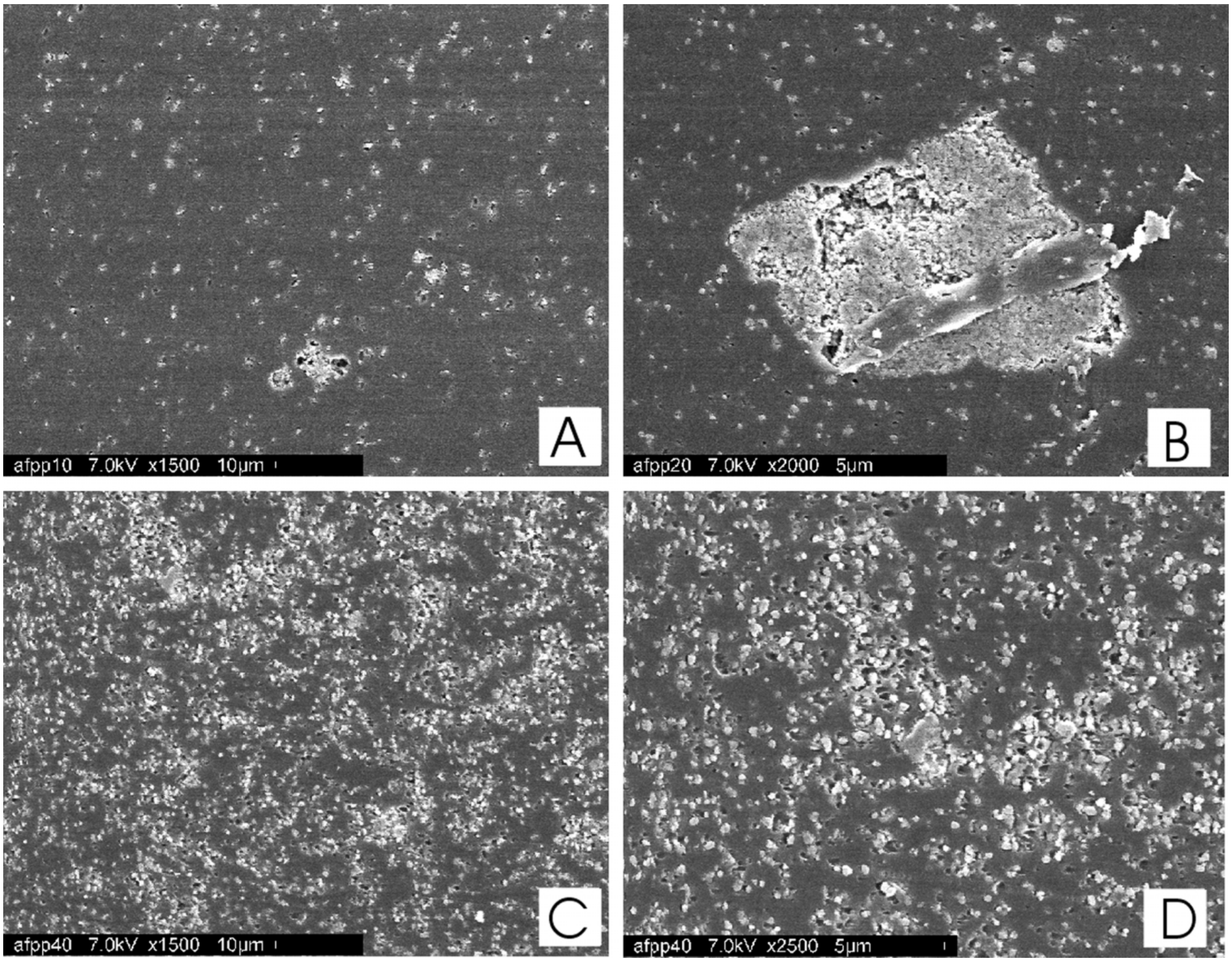

Fig. 14. Scanning electron microscope images of composite morphology, particle Type B; (A) 10 wt%; (B) 20 wt%; (C) 40 wt%; (D) 40 wt%.

aggregates are detrimental for the toughening properties of these composites [45]. The large aggregates create large voids upon loading and consequent debonding, and could function as precursors for cracks.

4.4. Thermal properties

The thermal properties have been determined by DSC, the results shown here are corrected for filler content, thus expressed in J/g polymer. In Fig. 15 the melting temperature and melting enthalpy are plotted as a function of particle content. It is shown that the melting temperature is constant at 164 °C for both the coated and uncoated particles. The melting enthalpy is also constant and remains at 80 J/g polymer for the coated particles. The untreated particles, however, interfere with the crystallisation process of the polypropylene phase. The melting enthalpy is lowered when the particle content is increased. The $CaCO_3$ particles do not act as a nucleating agent in polypropylene since the crystallinity is not increased.

4.5. Tensile properties

The influence of the interaction between filler particles and matrix polymer on the tensile properties is discussed in this section. Stiffness is one of the basic properties of composites and usually one of the main reasons to use a

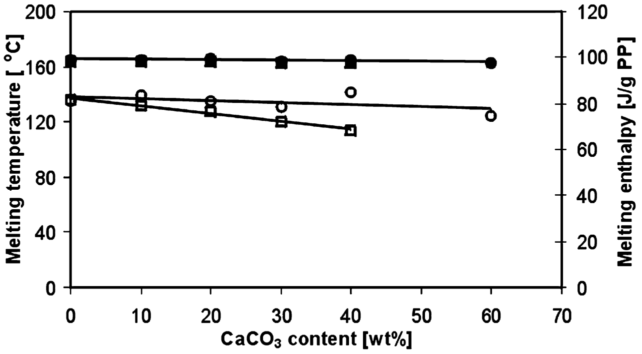

Fig. 15. Melting temperature and melting enthalpy as function of $CaCO_3$ content, ○, ΔH Treated $CaCO_3$ Type A; □, ΔH untreated $CaCO_3$ Type B; ●, T_m Treated $CaCO_3$ Type A; ■, T_m Untreated $CaCO_3$ Type B.

filler. The modulus is a low strain property. In this low strain regime the adhesion between particle and polymer remains intact. The interaction strength between polymer and particle has little effect on the modulus, the treated particles show approximately the same dependency on filler content as the untreated $CaCO_3$ particles (Fig. 16).

The yield stress is measured at considerable deformations, which lead to a complete different dependency of properties on fill fraction and particle–polymer interaction. The yield stresses are shown in Fig. 17 as a function of $CaCO_3$ content.

The tensile yield stress is lowered with particle content for both the coated and uncoated $CaCO_3$ particles. The yield point of the host matrix polymer is situated at 35 MPa and 8% strain at room temperature. At this strain level the particles have debonded or partially debonded from the polymer matrix. This leads to a lowering of the yield stress through the formation of voids, which do not contribute to the stress level. The tensile yield stress is raised if the particles do not debond from the polymer surface, as would be the case when the adhesion is very high. The surface treatment does not seem to be crucial for debonding to occur.

4.6. Impact properties

The impact performance depends on a number of local deformation mechanisms in the composite. The shear yielding of the host matrix polymer is the dominant energy consumer upon ductile fracture. Debonding of the particles changes the local stress state of the surrounding polymer and this reduces the sensitivity of the matrix polymer towards crazing and makes the yielding mechanism operative. The impact resistance is shown in Fig. 18 as a function of temperature.

Although the untreated particle composites have the same tensile properties as the treated particle composites it is clear that the toughening effect is lower. The particles treated with stearic acid show a larger increase in impact strength. The brittle-to-ductile transition temperature is shifted to a lower value for the coated $CaCO_3$ composites.

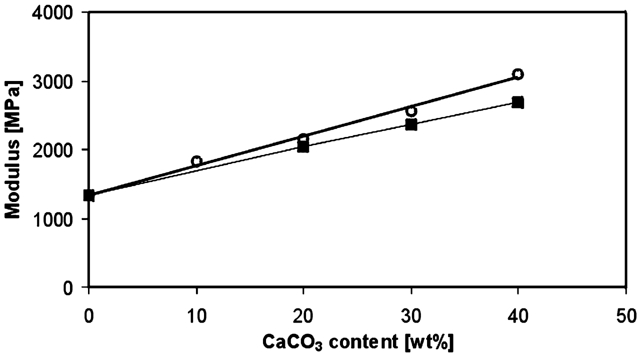

Fig. 16. Tensile modulus as function of particle content, 20 °C, 60 mm/min; ○, untreated $CaCO_3$ Type B; ■, Treated $CaCO_3$ Type A.

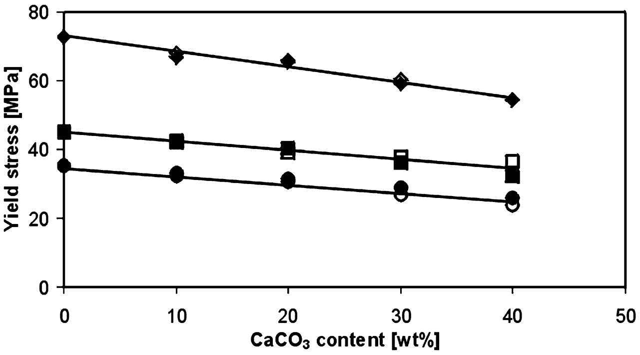

Fig. 17. Yield stress as a function of particle content, 60 mm/min, tensile, PP–$CaCO_3$ composites; ○, untreated 20 °C; ●, treated 20 °C; □, untreated 0 °C; ■, treated 0 °C; ◇, untreated − 30 °C; ◆, treated − 30 °C.

This effect is probably due to the poorer dispersion of the untreated $CaCO_3$ particles due to the higher particle–particle interactions. The polymer–particle interaction was not found to play an important role, because debonding was found to occur with both types of particles as was shown from the yield stress data.

5. Influence of particle size

5.1. Introduction

Although some contradictory data can be found in literature [2,56], it seems evident that the particle size has a pronounced effect on composite properties [57,58]. Strength and often modulus are increased, and deformability and impact strength decrease with decreasing particle size. Particle size in itself is not sufficient to characterise any filler, particle size distribution is equally important [57]. Large particles besides changing abrasion and appearance of the product usually have a strong adverse effect on the deformation and failure characteristics of the composite. The aggregation tendency increases with decreasing particle size [24,29]. Extensive aggregation leads towards insufficient homogeneity, rigidity and impact strength [2]. Clustered particles act as initiation sites in impact [2,16,45].

Different particles have been used to study the effect of

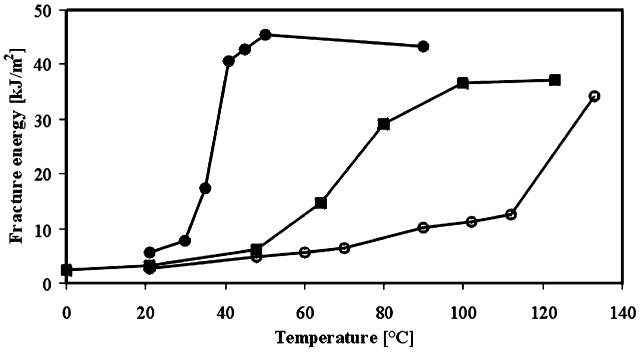

Fig. 18. Notched Izod fracture energy as function of temperature; ○, PP; ●, 30 wt% treated $CaCO_3$, Type A; ■, 30 wt% untreated $CaCO_3$, Type B.

coating and particle size. The particles used are: 0.07 μm untreated particles (Type C), 0.07 μm coated particles (Type D), 0.3 μm coated particles (Type E), 1.9 μm untreated particles (Type F).

5.2. Viscosity experiments

The melt viscosity is lowered to the same extent for both particle sizes, indicative of the degradation reactions occurring in the melt. The polypropylene melt is quite stable. The melt viscosity increases with decreasing particle size. Both composites in Fig. 19 are for untreated particles, the stearic acid treated particles showed the same trend in particle size. The higher melt viscosity of the smaller particles is indicative for the larger surface area of filler and consequently a larger interaction between polymer and particles.

5.3. Morphology

The morphology of composites of polypropylene with different particle sizes is shown in Fig. 20. The morphologies show coarse dispersion of particles in the PP matrix. There are aggregates visible, for all particle types. The dispersion is critical for these types of composites and apparently difficult to obtain. None of the filler particles show finely dispersed particles as was found for the 0.7 μm treated $CaCO_3$ particles. The particle–particle interactions of the untreated and small particles are too high for sufficient dispersion. The viscosity of the polypropylene could be too low to create large shear forces during extrusion. These obtained morphologies are not ideal for toughening the polypropylene matrix.

5.4. Thermal properties

PP is a semi-crystalline polymer and the crystallinity might be a function of $CaCO_3$ particle size. It is shown that the melting temperature is fairly constant with particle size. The melting enthalpy also remains unaffected by the particle size despite the larger surface area of the filler particles with decreasing particle size. The crystallinity of the polypropylene is constant for all composites shown in Fig. 21.

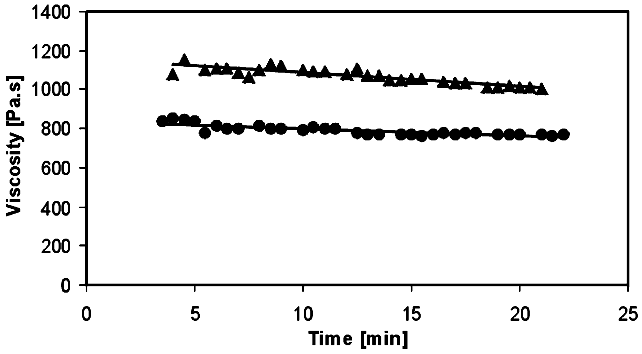

Fig. 19. Melt viscosity as a function of time, 270 °C, 1 mm/min; ●, 30 wt% 0.7 μm $CaCO_3$ untreated (Type B); ▲, 30 wt% 0.07 μm $CaCO_3$ untreated (Type A).

5.5. Tensile properties

The modulus is plotted as a function of particle size in Fig. 22.

The tensile modulus is unaffected by particle size for these polypropylene–$CaCO_3$ composites, the composites with stearic acid treated particles have somewhat lower moduli compared to the compounds with untreated particles.

The yield stress is measured at considerable deformations, which may lead to a different dependency of properties on particle size. The yield stresses are plotted as a function of particle size at a filler fraction of 30 wt% in Fig. 23. The decrease of the yield stress is due to the early debonding of the filler particles from the matrix polymer. Debonded particles do not contribute to the yield stress. The particle size does not seem to influence the tensile yield stress for these composites. Although debonding becomes increasingly more difficult with smaller particles [2] this is not seen in this particle size regime.

5.6. Impact properties

The notched fracture energy for the different particle sizes coated with stearic acid as a function of temperature is shown in Fig. 24. The impact strength at low temperatures is relatively low (5 kJ/m^2) and the fracture is macroscopically brittle. At elevated temperatures, the fracture becomes ductile and the impact strength is increased. The particle size shows an optimum in fracture energy at a particle size of 0.7 μm. The other particles show lower toughening levels, this is most likely due to the coarser morphology of those composites. The best balance of properties was reached with the stearic acid treated particles of 0.7 μm. The influence of the particle size of the uncoated particles on the impact fracture energy is shown in Fig. 25. The uncoated particles show a significant lower toughening effect compared to the treated particles. For the untreated particles the 0.7 μm particles also show the lowest brittle-to-ductile transition temperature.

6. Molecular weight effect of the matrix polymer

6.1. Introduction

The mechanical properties of PP composites depend on the morphology of the composite, the characteristics of the particles and matrix phase and the nature of the interface between these phases [59]. It has been shown that the dispersion of particles and with that the properties of blends and composites can be improved by increasing the molecular weight of the matrix polymer [59]. The improved

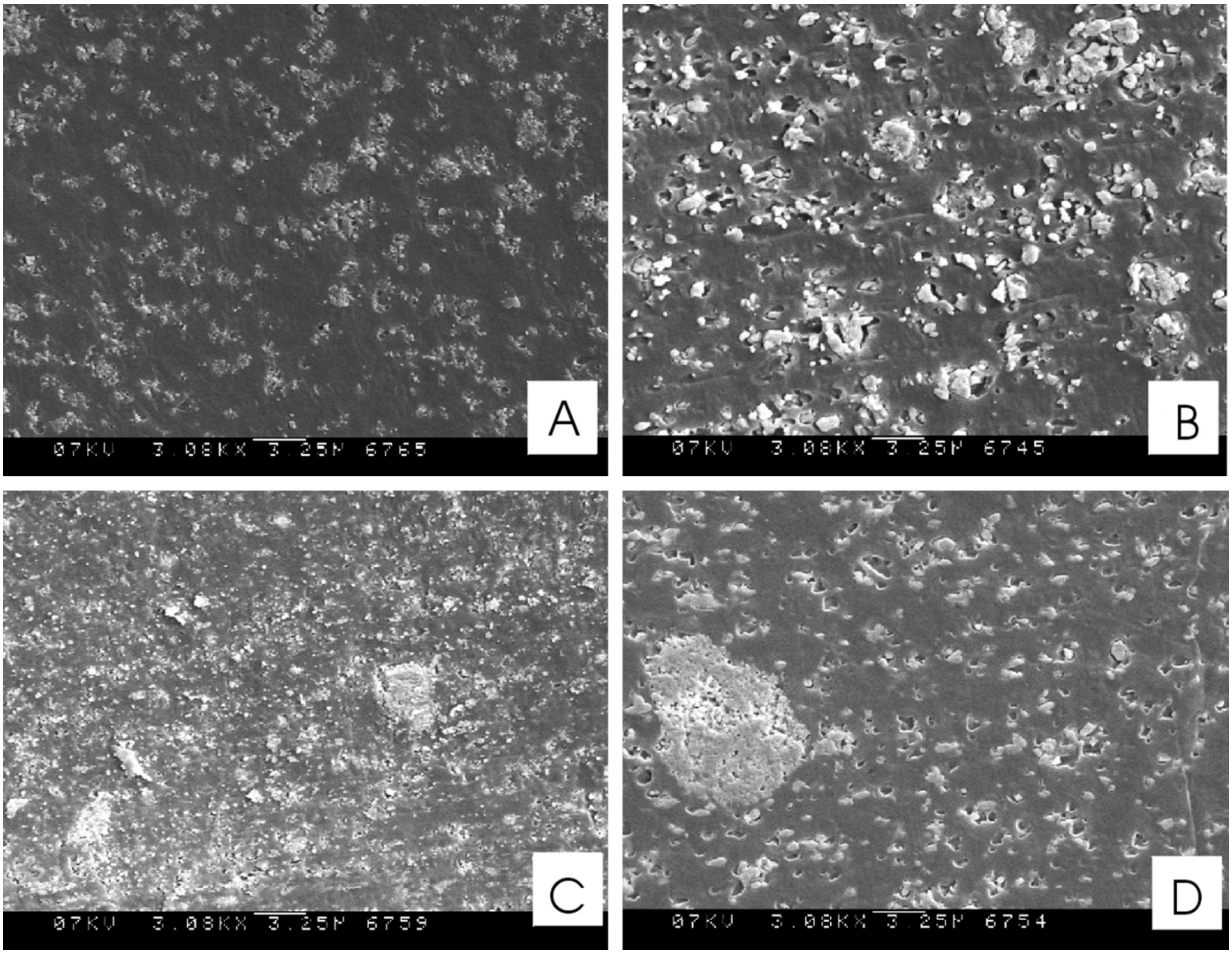

Fig. 20. SEM images of morphology of PP–$CaCO_3$ composites; (A) 0.07 μm untreated Type C; (B) 1.9 μm untreated Type F; (C) 0.07 μm treated Type D; (D) 0.3 μm treated Type E.

morphology stems from the increase in melt viscosity. Besides the influence on morphology it is known that an increase in molecular weight improves the inherent ductility, or the ability to be toughened of polymers [59].

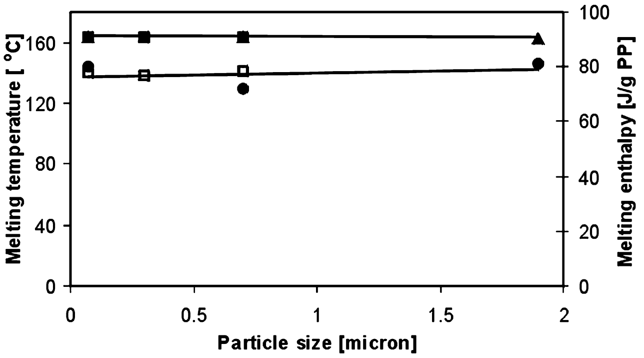

Fig. 21. Melting temperature and melting enthalpy as function of particle size, DSC 20 °C/min; 30 wt% PP–$CaCO_3$ composites, □, ΔH Coated particles; ●, ΔH uncoated particles; ■, T_m coated particles; ▲, T_m uncoated particles.

van der Wal and Gaymans [60] showed for polypropylene that an increase in molecular weight leads to a strong lowering of the brittle-to-ductile transition temperature. The molecular weight of the polypropylene matrix is varied here from MFI 24 to 0.3 dg/min (200,000 up to 657,000 g/mol). The particle content was kept at 30 wt% (Type A particles).

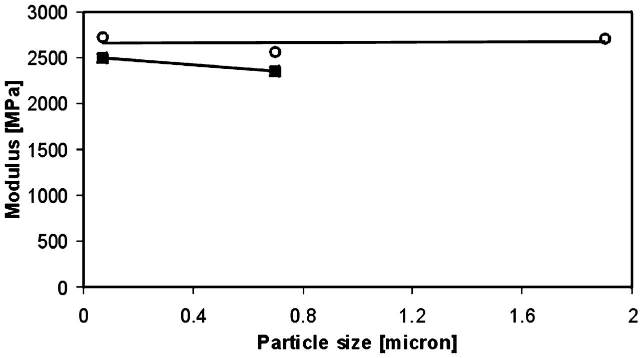

Fig. 22. Tensile modulus as function of particle size, 20 °C, 60 mm/min; ○, 30 wt% untreated particles; ■, 30 wt% treated particles.

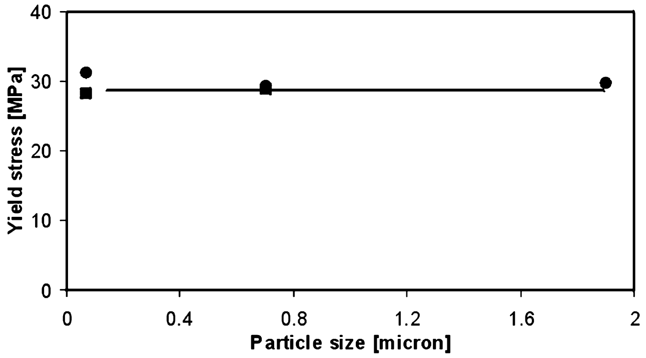

Fig. 23. Yield stress as a function of particle size, tensile, 20 °C, 60 mm/min; ■, 30 wt% untreated particles; ●, 30 wt% treated particles.

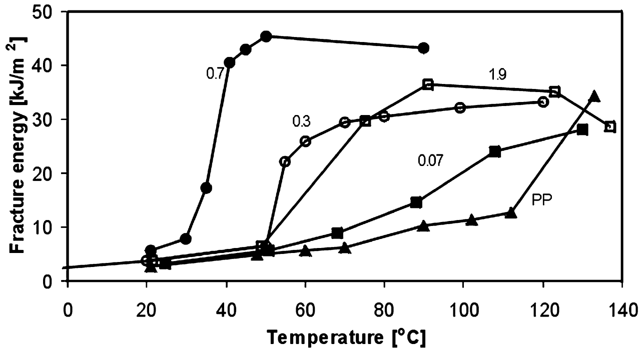

Fig. 24. Fracture energy as function of temperature, notched Izod, $CaCO_3$ particles, stearic acid treated; ▲, PP; ■, 0.07 μm; ○, 0.3 μm; ●, 0.7 μm; □, 1.9 μm.

6.2. Results

The notched Izod fracture energy is plotted as a function of temperature in Fig. 26. The influence of matrix molecular weight is obvious, an increase in matrix molecular weight leads to a strong increase in fracture energy.

The brittle-to-ductile transition temperature is lowered linearly with an increase in molecular weight (Fig. 27). This was also shown for the neat matrix polymer with an increase in molecular weight. The effect of particle content on the brittle-to-ductile transition is shown in Fig. 28 for two matrix polymers. The influence of molecular weight is to lower the complete curve of T_{bd} versus particle content. At the higher particle loading still a plateau value is reached only now at lower threshold temperature. It seems that even in this matrix polymer of higher molecular weight dispersion at higher filler contents is insufficient.

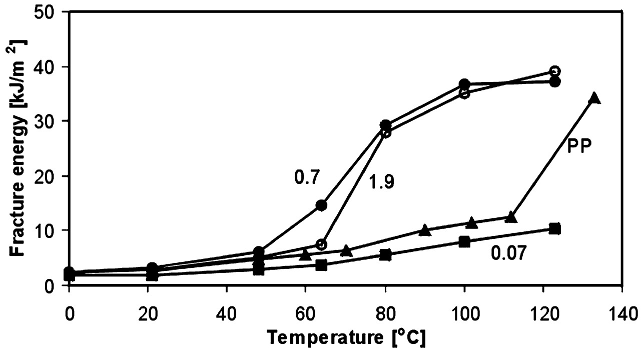

Fig. 25. Fracture energy as function of temperature, notched Izod, $CaCO_3$ particles, untreated; ▲, PP; ■, 0.07 μm; ●, 0.7 μm; ○, 1.9 μm.

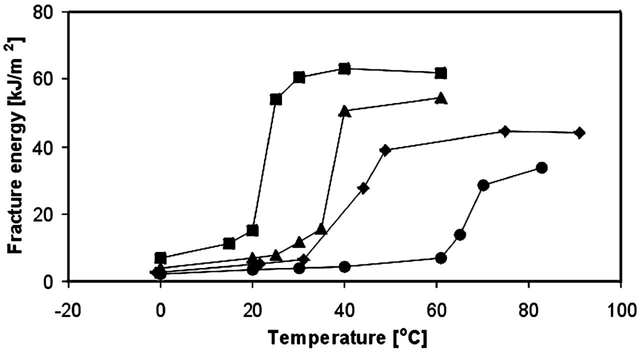

Fig. 26. Notched Izod fracture energy as a function of temperature, PP–$CaCO_3$ composites 30 wt%, Type A; ●, MFI: 24 dg/min; ◆, MFI: 2.4 dg/min; ▲, MFI: 1.1 dg/min; ■, MFI: 0.3 dg/min.

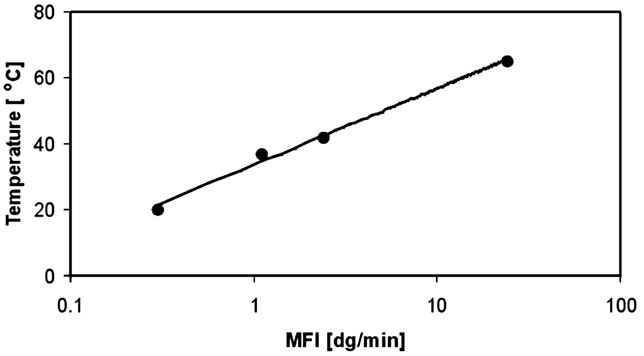

Fig. 27. Brittle-to-ductile transition temperatures as a function of matrix molecular weight, 30 wt% PP–$CaCO_3$ composites, Type A.

These composites with an increased molecular weight show that it is possible to obtain complete ductile fractures at room temperature (50–60 kJ/m^2) while the stiffness is increased simultaneously (Fig. 29).

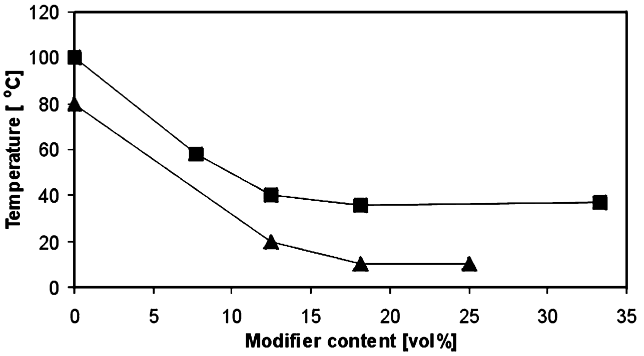

Fig. 28. Brittle-to-ductile transition temperatures as function of particle content Type A, notched Izod; ■, M_w 362,000 g/mol, MFI 2.4 dg/min; ▲, M_w 657,000 g/mol, MFI 0.3 dg/min.

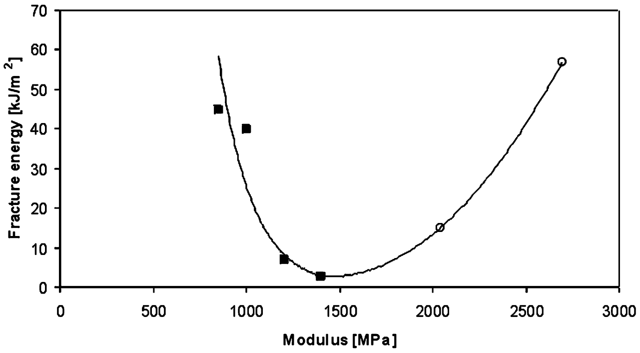

Fig. 29. Fracture energy as a function of modulus, 20 °C; ■, PP–EPDM; ○, PP–$CaCO_3$ (Type A).

7. Conclusions

The toughening of polypropylene with rigid particles leads to a system with higher stiffness and higher impact resistance (Fig. 29). The dispersion of the particles is critical in these composites and at high filler loads it may become difficult to avoid aggregates. Aggregates lead to less ductile behaviour. The shift of brittle-to-ductile transition temperature shows a limit at a filler load of 40 wt% of $CaCO_3$ particles. This is not caused by the glass transition of the polypropylene because the yield stress is still lowered at higher particle content and low temperatures. The dispersion could be a dominating factor in this threshold. When large aggregates are present the voids that are created by debonding are not stable and grow to a size where crack initiation occurs. The creation of stable free volume at the particle size level leads to high energy adsorption by shear yielding and consequently high impact resistance. Dispersion of the untreated particles was proved to be difficult and this had a detrimental effect on the impact properties. The smaller particles also were found to be less effective in toughening the polypropylene matrix due to a coarser morphology. The molecular weight of the polypropylene matrix had a profound effect on the toughening properties. A higher molecular mass shifted the brittle-to-ductile transition towards lower temperatures. At the higher filler loads, however, still problems seem to occur with dispersion, lowering the toughening efficiency. A polypropylene–$CaCO_3$ composite was processed which had a significant higher modulus and simultaneously showed improved toughness. The notched Izod impact energy could be raised from 2 to 50–60 kJ/m^2 at room temperature while increasing the modulus. Of all particle types used in this study, the stearic acid treated particles of 0.7 μm were found to give the best combination of properties. It is expected that the stearic acid coating used in this study is not yet optimal for toughening polypropylene, the impact properties can be increased even further by optimising the surface treatment of the $CaCO_3$ particles.

Acknowledgements

This research was financed by the Shell Research and Technology Centre Amsterdam. The authors would like to thank P.J. Fennis and A.A. Smaardijk for their contribution and helpful discussions.

References

[1] Bartczak Z, Argon AS, Cohen RE, Weinberg M. Polymer 1999;40:2347.
[2] Pukánszky B. In: Karger-Kocsis J, editor. Polypropylene: structure, blends and composites. London: Chapman & Hall; 1995. Chapter 1.
[3] Kim GM, Michler GH. Polymer 1998;39:5689.
[4] Baker RA, Koller LL, Kummer PE. Handbook of fillers for plastics, 2nd ed. New York: Van Nostrand Reinhold; 1987.
[5] Wang Y, Lu J, Wang GJ. J Appl Polym Sci 1997;64:1275.
[6] Hoffmann H, Grellmann W, Zilvar V. Polymer composites. New York: Walter de Gruyter; 1986.
[7] Badran BM, Galeski A, Kryszewski M. J Appl Polym Sci 1982;27:3669.
[8] Liu ZH, Kwok KW, Li RKY, Choy CL. Polymer 2002;43:2501.
[9] Thio YS, Argon AS, Cohen RE, Weinberg M. Polymer 2002;43:3661.
[10] Zuiderduin WCJ, Westzaan C, Huétink J, Gaymans RJ. Antec 2001 SPE, ISBN 1-56676-804-7, 2848–52.
[11] Zuiderduin WCJ, Westzaan C, Huétink J, Gaymans RJ. Antec 2001 SPE, ISBN 1-56676-804-7, 3493–97.
[12] Greco R, Coppola F. Plast Rubber Process Appl 1986;6:35.
[13] Kowaleski T, Galeski A. J Appl Polym Sci 1986;32:2919.
[14] Maurer FHJ, Schoffeleers HM, Kosfeld R, Uhlenbroich T. Analysis of polymer filler interaction in filled polyethylene. Progress in science and engineering of composites. Tokyo: ICCM-IV; 1982. p. 803.
[15] Burton RH, Day TM, Folkes MJ. Polym Commun 1984;25:361–2.
[16] Riley AM, Paynter CD, McGenity PM, Adams JM. Plast Rubber Process Appl 1990;14:85.
[17] Folkes MJ, Hardwick ST. J Mater Sci Lett 1987;6:656–8.
[18] Goodier JN. J Appl Mech 1933;55:39.
[19] Kowaleski T, Galeski A, Kryszewski M. Polymer blends, processing, morphology and properties. New York: Plenum Press; 1984. p. 223.
[20] Mencel J, Varga J. J Therm Anal 1983;28:161.
[21] Nakagawa H, Sano H. Polym Prepr 1985;26:249.
[22] Bucknall CB. In: Paul DR, Bucknall CB, editors. Polymer blends: performance, vol. 2. New York: Wiley; 2000. Chapter 22.
[23] Varga J. J Therm Anal 1989;35:1891.
[24] Svehlova V, Poloucek E. Angew Makromol Chem 1987;153:197.
[25] Yue CY, Cheung WL. J Mater Sci 1991;26:870.
[26] Ramsteiner F, Theyson R. Composites 1984;15:121.
[27] Gasleski A, Kalinski R, Polymer blends, processing, morphology and properties, vol. 1. New York: Plenum Press; 1980. p. 431.
[28] Vollenberg PHT, Heikes D. Polymer 1989;30:1656.
[29] Suetsugu Y, White JL. Adv Polym Technnol 1987;7:427.
[30] Jancar J, Kucera J. Polym Engng Sci 1990;30:707.
[31] Fekete E, Pukansky B, Toth A, Bertoti I. J Colloid Interf Sci 1990;135:200.
[32] Papirer E, Schultz J, Turchi C. Eur Polym J 1984;12:1155.
[33] Vu-Kahn T, Fisa B. Polym Compos 1986;7:219.
[34] Allard R, Vu-Kahn T, Chalifoux JP. Polym Compos 1989;10:62.
[35] Bucknall CB. Toughend plastics. London: Applied Science; 1977.
[36] Michler GH, Starke JU. In: Riew CK, Kinloch AJ, editors. Toughend plastics. II. Science and engineering. Washington, DC: American Chemical Society; 1996. p. 251.
[37] Michler GH. Kunstoff-Mikromechanik: morphologie, deformations- und Bruch-mechanismen. Munich: Carl Hanser; 1992.
[38] Yee AF, Maxwell M. Polym Engng Sci 1981;21:5.

[39] Kramer EJ. Adv Polym Sci 1983;52/53:1.

[40] Rowe EH, Riew CK. Plast Engng 1975;31:45.

[41] Sutton NJ, McGarry F. J Polym Engng Sci 1973;13:29.

[42] Riew CK, Rowe EH, Siebert AR. Toughness and brittleness of plastics. Advances in Chemistry Series No. 154, Washington: American Chemical Society; 1976.

[43] Ahmad ZB, Ashyby MF, Beaumount PWR. Scr Metall 1986;20:843.

[44] Parker DS, Sue HJ, Huang J, Yee AF. Polymer 1990;31:2267.

[45] Michler GH, Tovmasjan JM. Plaste Kautschuk 1988;35:73.

[46] van der Wal A, Nijhof R, Gaymans RJ. Polymer 1999;40:6031.

[47] Gaymans RJ. In: Paul DR, Bucknall CB, editors. Polymer blends: performance, vol. 2. New York: Wiley; 2000. p. 177. Chapter 25.

[48] Zuiderduin WCJ, Gaymans RJ. Submitted for publication.

[49] Ramsteiner F, Heckmann W. Polym Commun 1985;26:199.

[50] Gaymans RJ, Borggreve RJM, Oostenbrink AJ. Makromol Chem 1990;38:125.

[51] Speroni F, Castoldi E, Fabbri P, Casiraghi T. J Mater Sci 1989;24:2165.

[52] Oostenbrink AJ, Dijkstra K, vander Wal A, Gaymans RJ. P.R.I. Conference Cambridge; 1990, paper 50.

[53] Boode JW, Gaalman AEH, Pijpers AJ, Borggreve RJM. Poster presented at the Prague Macromolecular Meetings; 1990.

[54] Dijkstra K, Wevers HH, Gaymans RJ. Polymer 1994;35:323.

[55] van der Wal A. The fracture behavior of polypropylene and polypropylene–rubber blends. Thesis University of Twente, 1996; chapter 8.

[56] Schlumpf HP. Modern aspects of fillers in polypropylene, presented at the 10th International Macromolecule Symposium, 20–21 September, 1990, Interlaken, Switzerland.

[57] Schlumpf HP, Bilogan W. Kunstoffe 1983;71:820.

[58] Schmidt H, Jzquierdo R. Kunstoffe 1988;78:149.

[59] Oshinski AJ, Keskkula H, Paul DR. Polymer 1996;37:4909.

[60] van der Wal A, Mulder JJ, Thijs HA, Gaymans RJ. Polymer 1998;39:5467.